J. Fluid Mech. (1980), vol. 97, part 1, pp. 157–179
Printed in Great Britain

An approximate method for solving two-dimensional low-Reynolds-number flow past arbitrary cylindrical bodies

By H. YANO

Department of Mechanical Engineering, Maizuru Technical College, 625 Japan

AND A. KIEDA

Department of Mechanical Engineering, Doshisha University, Kyoto, 602 Japan

(Received 28 February 1978 and in revised form 2 July 1979)

This paper presents an approximate method for solving Oseen's linearized equations for a two-dimensional steady flow of incompressible viscous fluid past arbitrary cylindrical bodies at low Reynolds numbers. The formulation is based on a discrete singularity method with a least squares criterion for satisfying the no-slip boundary condition. That is, sets of Oseenlets, sinks, sources and vortices are discretely distributed in the interior of the body, and then the least squares criterion attempts to minimize the integrated squares of velocities along the body contour, thus leading to a system of simultaneous algebraic equations. Complex-variable arithmetic, usually available on modern computers, makes the computation algorithm very simple. Furthermore, the method is applicable to cases that cannot be solved by classical analytical approaches. As examples of application, we computed the forces acting on a single circular cylinder, two circular cylinders of equal radius separated by a distance, an inclined elliptic cylinder and an inclined square cylinder all of which are immersed in uniform flow fields. The computed results agree very well with those of classical analytical methods.

1. Introduction

As is well known, the behaviour of a steady uniform flow of incompressible viscous fluid past obstacles is governed approximately by the Oseen's equations of motion proposed by Oseen (1910), provided that the Reynolds number of the flow field is fairly small. Strictly speaking, Oseen's equations are not valid in regions very near to body surfaces, but it is generally recognized that the so-called homogeneous Oseen flow which obeys Oseen's equations everywhere in the field, is a useful model to calculate approximately the forces acting on obstacles in low-Reynolds-number flow.

Since Oseen's proposal, various analytical investigations have been hitherto made to solve flow problems of this type. However, analytical solutions have been found only for special geometries. For example, Lamb (1911) (see also Lamb 1932) first proposed the famous formula for the drag acting on a single circular cylinder placed in an oncoming uniform flow. Bairstow (1923) extended Lamb's formula to obtain an analytical expression for the drag on an elliptic cylinder with its major axis parallel to the undisturbed flow. Furthermore, Faxén (1927) gave the exact solution for the case of a

0022-1120/80/4393-8390 $02.00

circular cylinder. And Filon (1926) established general formulae for the drag and lift experienced by an arbitrary cylindrical body in terms of the inflow along its wake, and the circulation around it. Later, Imai (1951) refined Filon's theory, and also presented a formula for the moment acting on a cylindrical body. In addition, Imai (1954) developed a general method of solving two-dimensional Oseen equations by making use of complex variables and analytic functions.

In general, these classical approaches are included in the ordinary boundary-value method which is based on the choice of an appropriate co-ordinate system according to the body geometry in question. And so body geometries to be dealt with are somewhat restricted. On the other hand, for potential flow problems, another method known as the singularity method has already been developed to seek solutions for more complicated geometries, and various techniques have been proposed for the types of singularities and their spatial distributions both in the two-dimensional and three-dimensional cases. Hess & Smith (1966) presented a typical formulation where singularities with unknown strengths are distributed continuously on the body boundaries, and then the boundary conditions are reduced to simultaneous algebraic equations for the unknown strengths of singularities. This method has been extended by Youngren & Acrivos (1975) to the case of Stokes flows. They had an unknown distribution of Stokeslets over the body boundaries, and obtained their strengths numerically by solving a system of linear algebraic equations.

Recently, the present authors Kieda & Yano (1978) developed a discrete singularity method with the least squares criterion for the two-dimensional potential flow problem. The present method is in fact an extension of this discrete singularity technique to the case of low-Reynolds-number flow. That is, with the problem restricted to the case of two-dimensional external flows, we first have a discrete distribution of sets of Oseenlets, sources, sinks and vortices in the interior of the obstacle, and then apply the least squares criterion to the no-slip boundary condition, thus obtaining a system of linear equations for the unknown strengths of the singularities, which can be solved numerically with the use of a computer. This formulation is basically a numerical approach with a very simple computation algorithm because of the use of complex variables. In addition, it gives an approximate analytical expression for the complex velocity in a much easier-to-tackle form than any that can be found in the continuous singularity technique.

2. General solution of Oseen's equations

The starting point of the present method is Oseen's linearized equations for two-dimensional steady flows of incompressible viscous fluids expressed as

$$U_\infty \frac{\partial u}{\partial x} = -\frac{1}{\rho}\frac{\partial p}{\partial x} + \nu\nabla^2 u, \tag{2.1}$$

$$U_\infty \frac{\partial v}{\partial x} = -\frac{1}{\rho}\frac{\partial p}{\partial y} + \nu\nabla^2 v, \tag{2.2}$$

where $\nabla^2 = \partial^2/\partial x^2 + \partial^2/\partial y^2$, x and y being the Cartesian co-ordinates, u and v the velocity components along x and y respectively, U_∞ the velocity at infinity in the direction of x axis, p the pressure, ρ the density, and finally ν the kinematic viscosity. And the equation of continuity is

$$\partial u/\partial x + \partial v/\partial y = 0. \tag{2.3}$$

It is generally recognized that Oseen's equations (2.1) and (2.2) which approximate the nonlinear convective terms of the full Navier–Stokes equations are usually valid for Reynolds numbers of less than 1 in the sense of order except in regions very near to obstacles, where the Reynolds number is based on the body size. However, in predicting practically the total forces experienced by immersed bodies, we can expect that Oseen's equations are sometimes effective for Reynolds numbers even more than 1, as will be later argued in the case of a circular cylinder.

Imai (1954) (see also Rosenhead 1963) solved (2.1) and (2.2) with (2.3) to obtain the general expression for the complex velocity $W = u - iv$ in the form

$$W = e^{\lambda x} \sum_{n=0}^{\infty} K_n(\lambda r)\,(\bar{A}_{n+1} e^{in\theta} + A_n e^{-in\theta}) + f(z), \tag{2.4}$$

with

$$\lambda = U_\infty/2\nu, \tag{2.5}$$

where $r = |z|$, $\theta = \arg(z)$ and $z = x + iy$. In addition, K_n are the modified Bessel functions of the second kind, and $f(z)$ is an arbitrary analytic function of z which expresses the complex velocity of the potential flow.

3. Approximate method of solution

Now, to seek a particular solution of Oseen's equations, we insert into (2.4)

$$A_1 = a^{(1)} + ia^{(2)},$$

$$A_n = 0 \quad n \neq 1,$$

and

$$f(z) = (a^{(3)} + ia^{(4)})/\lambda z,$$

and arrive at

$$W_e = \sum_{k=1}^{4} a^{(k)} W_e^{(k)}, \tag{3.1}$$

where

$$W_e^{(1)} = e^{\lambda x}\{K_0(\lambda r) + K_1(\lambda r)\,e^{-i\theta}\}, \tag{3.2}$$

$$W_e^{(2)} = ie^{\lambda x}\{-K_0(\lambda r) + K_1(\lambda r)\,e^{-i\theta}\}, \tag{3.3}$$

and

$$W_e^{(3)} = 1/\lambda z, \quad W_e^{(4)} = i/\lambda z. \qquad (3.4), (3.5)$$

As is well known, the so-called Oseenlet is such that it causes a complex velocity

$$W_0 = a^{(1)}\{W_e^{(1)} - W_e^{(3)}\} + a^{(2)}\{W_e^{(2)} - W_e^{(4)}\}. \tag{3.6}$$

Then, it can be considered that the perturbation velocity W_e occurs owing to a composite singularity, a set of an Oseenlet, source or sink, and vortex located at the origin of the co-ordinate system in an unbounded uniform flow field with the velocity U_∞.

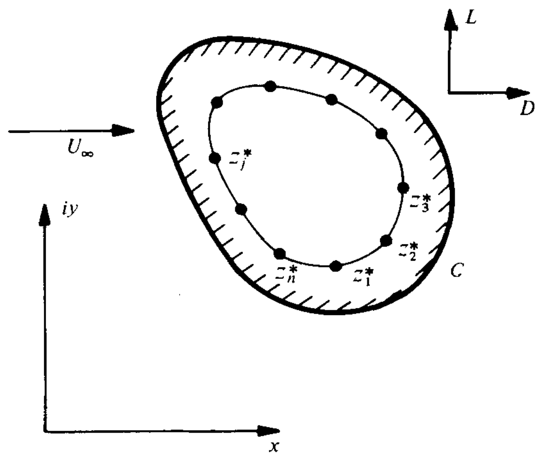

FIGURE 1. Flow past an arbitrary cylindrical body. z_j^*, position of a composite singularity.

Filon's formulae (1926) states that the force acting on the Oseenlet immersed in a uniform flow U_∞ is given by

$$X_0 + iY_0 = -4\pi\mu\{a^{(1)} + ia^{(2)}\}, \tag{3.7}$$

where μ designates the coefficient of viscosity of the fluid. On the other hand, it is easy to show that the singularities other than the Oseenlet, as a whole, experience the force

$$X_1 + iY_1 = 4\pi\mu\{a^{(1)} + a^{(3)} - ia^{(2)} - ia^{(4)}\}. \tag{3.8}$$

From (3.7) and (3.8), we obtain the expressions for the drag D_e and lift L_e acting on the composite singularity located in an oncoming uniform flow U_∞, namely

$$D_e = X_0 + X_1 = -4\pi\mu\{2a^{(1)} + a^{(3)}\}, \tag{3.9}$$

$$L_e = Y_0 + Y_1 = 4\pi\mu a^{(4)}. \tag{3.10}$$

Furthermore, the outflow Q_e from this singularity can be expressed by

$$Q_e = \frac{2\pi}{\lambda}\{a^{(1)} + a^{(3)}\}, \tag{3.11}$$

because there is no outflow from the Oseenlet as is obvious from Filon's discussion (1926).

Owing to the linearity of Oseen's equations (2.1) and (2.2), it is possible to take a discrete distribution of composite singularities of number n located at $z_1^*, z_2^*, \ldots, z_n^*$ inside the cylindrical body. And, in the present method, we propose a practical and comparatively general assumption that the singularities should be placed on the contour of a geometry similar to the body boundary with their centroids being coincident, as is illustrated in figure 1. They perturb the uniform flow U_∞ to cause a complex velocity in the form

$$W = U_\infty + \sum_{j=1}^{n} \sum_{k=1}^{4} a_j^{(k)} W_j^{(k)}, \tag{3.12}$$

where

$$W_j^{(1)} = e^{\lambda x_j}\{K_0(\lambda r_j) + K_1(\lambda r_j)\, e^{-i\theta_j}\}, \tag{3.13}$$

$$W_j^{(2)} = ie^{\lambda x_j}\{-K_0(\lambda r_j) + K_1(\lambda r_j)\, e^{-i\theta_j}\}, \tag{3.14}$$

$$W_j^{(3)} = 1/\lambda z_j, \quad W_j^{(4)} = i/\lambda z_j, \qquad (3.15), (3.16)$$

and $z_j = z - z_j^*$, $r_j = |z_j|$, $\theta_j = \arg(z_j)$.
Letting $W_l^* = W_j^{(k)}$ and $a_l^* = a_j^{(k)}$ with $l = j + (k-1)\, n$, we get

$$W = U_\infty + \sum_{l=1}^{4n} a_l^* W_l^*. \tag{3.17}$$

On the other hand, in order to satisfy the no-slip boundary condition approximately on the body contour, the least squares criterion attempts to minimize a parameter I defined by

$$I = \oint_C W\overline{W} ds, \tag{3.18}$$

where C represents the body contour, and s designates a curvilinear co-ordinate along the contour. From this minimization, it follows that

$$\partial I/\partial a_j^* = 0 \quad j = 1, 2, \ldots, 4n. \tag{3.19}$$

Substituting (3.17) and (3.18) into (3.19), we have

$$\oint_C (W\overline{W}_j^* + \overline{W} W_j^*)\, ds = 0, \quad j = 1, 2, \ldots, 4n, \tag{3.20}$$

which leads to the following matrix form:

$$\mathbf{G}\mathbf{a}^* = \mathbf{b}, \tag{3.21}$$

where

$$\left.\begin{aligned} G_{jk} &= \oint_C \{\mathscr{R}(W_j^*)\mathscr{R}(W_k^*) + \mathscr{I}(W_j^*)\mathscr{I}(W_k^*)\}\, ds, \\ b_j &= -U_\infty \oint_C \mathscr{R}(W_j^*)\, ds, \end{aligned}\right\} \quad \begin{aligned} j &= 1, 2, \ldots, 4n, \\ k &= 1, 2, \ldots, 4n. \end{aligned}$$

To obtain the complex velocity W, we have to determine the $4n$ unknowns a_j^* numerically from the system of linear equations (3.21) with the aid of a computer. Fortunately, the computation of G_{jk} and b_j is very easy because of the availability of complex-variable arithmetic in a modern computer.

Moreover, it is natural that the similarity ratio between the body boundary and the singularity-located contour should be determined so as to minimize the integral I.

Then, referring to (3.9) and (3.10), we can find approximate expressions for the drag D and lift L acting on the cylindrical body in question, namely

$$D \cong -4\pi\mu\left(2 \sum_{j=1}^{n} a_j^* + \sum_{j=2n+1}^{3n} a_j^*\right), \tag{3.22}$$

$$L \cong 4\pi\mu \sum_{j=3n+1}^{4n} a_j^*, \tag{3.23}$$

if the parameter I is small enough to satisfy the no-slip boundary condition approximately.

Remembering (3.11), this assumption of the minimization of I down to a sufficiently small value also yields

$$Q = \frac{2\pi}{\lambda}\left(\sum_{j=1}^{n} a_j^* + \sum_{j=2n+1}^{3n} a_j^*\right) \cong 0, \tag{3.24}$$

where Q is regarded as a residual of the outflow from the obstacle which may occur in such an approximate approach as the present one. Thus, we rewrite (3.22) as

$$D \cong 4\pi\mu \sum_{j=2n+1}^{3n} a_j^*. \tag{3.25}$$

Hence, the drag and lift coefficients are

$$C_D = \frac{2\beta D}{\rho U_\infty^2 l} \cong \frac{8\alpha\beta}{U_\infty Re} \sum_{j=2n+1}^{3n} a_j^*, \tag{3.26}$$

$$C_L = \frac{2\beta L}{\rho U_\infty^2 l} \cong \frac{8\pi\beta}{U_\infty Re} \sum_{j=3n+1}^{4n} a_j^*, \tag{3.27}$$

with

$$Re = U_\infty l/\nu, \tag{3.28}$$

where Re denotes the Reynolds number based on a representative length l, and β depends on the definition of C_D and C_L.

Lastly, we shall try to estimate roughly errors occurring in thus computed drag and lift coefficients. Considering Filon's formulae, the error ΔD in the calculated drag can be reasonably supposed as

$$|\Delta D| = O(\rho U_\infty^2 I^* S_0), \tag{3.29}$$

where

$$I^* = \frac{1}{U_\infty}\left(\frac{I}{S_0}\right)^{\frac{1}{2}}, \tag{3.30}$$

with S_0 being the perimeter of the obstacle. This is because the residual of the total outflow at infinity excluding the wake is assumed to be of the order of $U_\infty I^* S_0$. Hence, recalling (3.26), we have

$$\begin{aligned} |\Delta C_D| &= \frac{2\beta}{\rho U_\infty^2 l}|\Delta D| \\ &= O(2\beta S_0 I^*/l). \end{aligned} \tag{3.31}$$

Similarly, the error in the computed lift coefficient can be estimated as

$$|\Delta C_L| = O(2\beta S_0 I^*/l). \tag{3.32}$$

However, it is considered that the validity of this error estimation should be further examined in the future from another point of view.

4. Numerical discussions

4.1. *Drag acting on a single circular cylinder*

We shall compute the drag experienced by a single circular cylinder of radius a immersed in an unbounded uniform flow field.

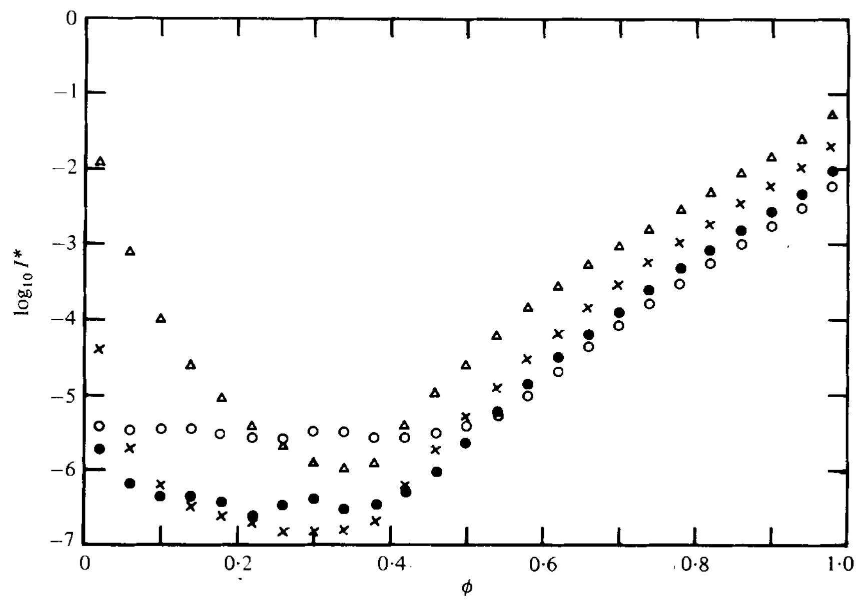

FIGURE 2. Values of I^* plotted against similarity ratio ϕ, in the case of a single circular cylinder. ○, $Re = 0{\cdot}01$; ●, $Re = 0{\cdot}1$; ×, $Re = 1$; △, $Re = 5$.

First, with twelve singularities placed on a concentric circle of radius $\delta = \phi a$, where ϕ is a similarity ratio, values of I^* are calculated within a range of $0 < \phi < 1$, using a trapezoidal rule with division number $N = 100$. The results are plotted in figure 2 in terms of the Reynolds number $Re = 2aU_\infty/\nu$ as a parameter. This figure indicates that the optimum value of ϕ which minimizes I^*, is nearly 0·3, being almost independent of Re within the range of $0{\cdot}01 \leqslant Re \leqslant 5$. This is very favourable for the present formulation.

The drag coefficients C_D based on $l = 2a$ and $\beta = 1$ in equation (3.26) are computed for various Reynolds numbers Re up to 4, with a similarity ratio of 0·3. The results are shown in figure 3, compared with the existing expansion formulae and Tritton's experiments (1959). These formulae are expressed as

$$\text{(i)}\ C_D = \frac{8\pi}{ReT_1}, \tag{4.1}$$

$$\text{(ii)}\ C_D = \frac{8\pi}{Re\,T_1}(1-T_2), \tag{4.2}$$

$$\text{(iii)}\ C_D = \frac{8\pi}{Re\,T_1}\left\{1-T_2-\frac{Re^4}{32^2T_1^2}\left(T_1^4-\tfrac{1}{3}T_1^3+\tfrac{2}{72}T_1-\tfrac{25}{256}\right)\right\}, \tag{4.3}$$

where

$$T_1 = \tfrac{1}{2}-\gamma-\ln\frac{Re}{8}, \quad T_2 = \frac{Re}{32T_1}\left(T_1^2-\tfrac{1}{2}T_1+\tfrac{5}{16}\right),$$

and $\gamma = 0{\cdot}57721\,\ldots$ (Euler's constant). The first one is Lamb's (1911), and the second and third are Tomotika & Aoi's (1951), which are all based on the homogeneous

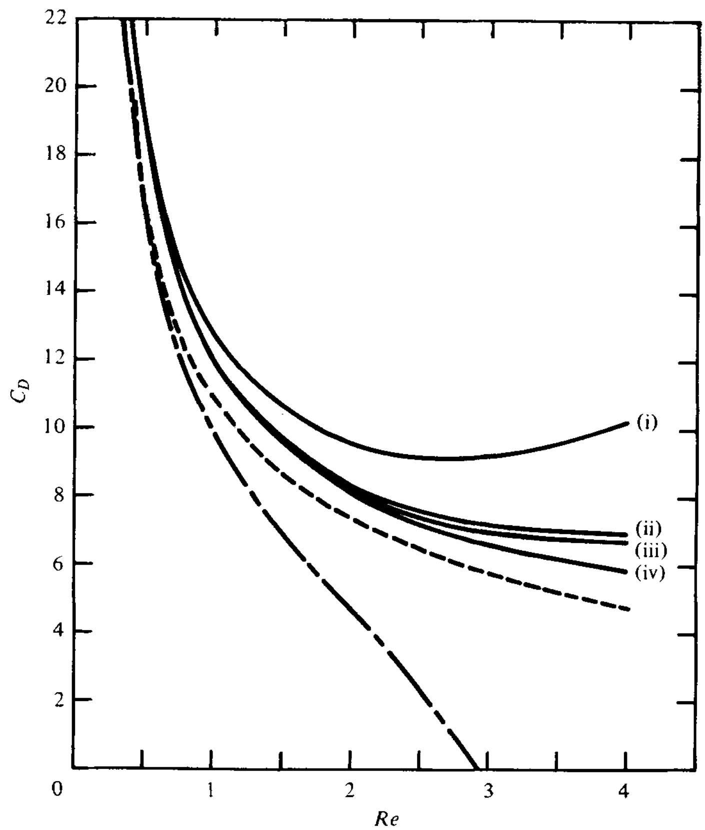

FIGURE 3. Drag coefficients C_D for a single circular cylinder, plotted against Reynolds number Re. (i) Lamb's equation (4.1); (ii) Tomotika's equation (4.2); (iii) Tomotika's equation (4.3); (iv), present results; ——, Kaplun's equation (4.4); ------, Tritton's experiment (1959).

Oseen's equations. Further, we quote Kaplun's approximation (1957) in the form

$$C_D = \frac{8\pi}{ReT_1}(1 - 0{\cdot}87T_1^{-2}), \tag{4.4}$$

which is plotted in figure 3. It was derived from the famous method of matched asymptotic expansions with inner Stokes flow and outer Oseen flow.

As is obvious from figure 3 or after Van Dyke (1964), Kaplun's is closest to Tritton's experiments for $Re < 1$. And its limited utility is understood to be mainly due to the truncation of the series of T_1. However, among the others, the present results indicated by (iv) agree most closely with Tritton's data for $Re < 4$. It is especially noticeable that there is a comparatively good agreement between them at as high a Reynolds number as $Re = 4$ where the flow near to the obstacle actually obeys the full Navier–Stokes equations, not Oseen's equations. In other words, it can be expected that a highly accurate solution for the homogeneous Oseen's equations is sometimes useful even outside the so-called low-Reynolds-number range $Re < 1$, so long as we concern the total force acting on a body. Besides, the solution can be used as the initial approximation of a possible iterative procedure for solving the full Navier–Stokes

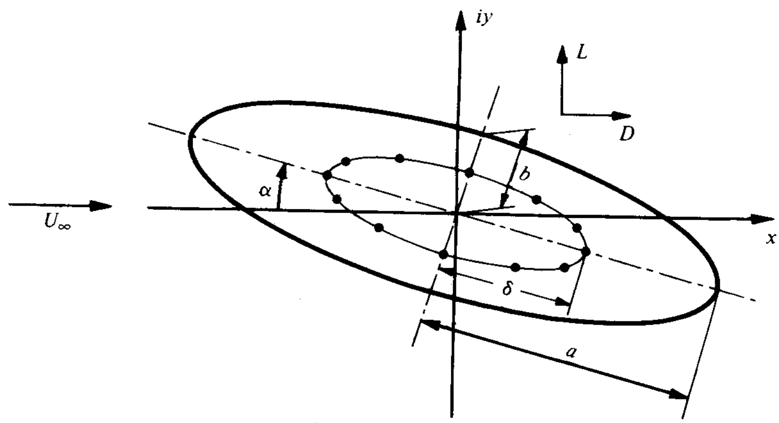

FIGURE 4. Flow past an inclined elliptic cylinder. ●, position of a composite singularity.

equations. For this reason, some of the computations in the present paper cover a wide Reynolds-number range up to $Re = 5$.

Additionally, from (3.31) with the data illustrated in figure 2, the error in the computation of C_D can be estimated to be of the order of less than 10^{-5} over the entire range of Re, if only Oseen's approximation is assumed.

4.2. *Forces acting on an inclined elliptic cylinder*

We now proceed to compute the drag D and lift L experienced by an elliptic cylinder of major axis $2a$ and minor axis $2b$, inclined at an arbitrary angle α in an oncoming uniform flow U_∞, as is shown in figure 4. In this case, twelve composite singularities are located inside the body the same as before.

Then, with $l = 2a$ and $\beta = 1$ in (3.26)–(3.28), we can define

$$C_D = D/\rho U_\infty^2 a, \quad C_L = L/\rho U_\infty^2 a, \tag{4.5), (4.6}$$

and

$$Re = 2aU_\infty/\nu. \tag{4.7}$$

Figures 5 and 6 present variations of I^* with the similarity ratio $\phi = \delta/a$ at $\alpha = 0°$; the former being for $t = 0{\cdot}1$ and the latter for $t = 0{\cdot}5$, where $t = b/a$. They show characteristics like those for a circular cylinder illustrated in figure 2. That is, the optimum values of ϕ are almost independent of the Reynolds number in the range of

$$0{\cdot}01 \leqslant Re \leqslant 5,$$

and hardly affected by the angle of attack α, though the data are omitted in the present paper. Then, we employ $\phi = 0{\cdot}96$ for $t = 0{\cdot}1$ and $\phi = 0{\cdot}8$ for $t = 0{\cdot}5$ in numerical calculations. Additionally, for the optimum similarity ratios, I^* decreases with Re. And so, it can be expected that solutions at lower Reynolds numbers are more accurate than ones at higher Reynolds numbers.

Computed drag and lift coefficients are plotted in figures 7 through 10 for thickness ratios $t = 0{\cdot}1$, $0{\cdot}5$ and $1{\cdot}0$, and $Re = 0{\cdot}1$ and $1{\cdot}0$, compared with Imai's results (1954) (see also Rosenhead 1963) found in an approximate analytical method; figures 7 and 8 being for the drag coefficient C_D, and figures 9 and 10 for the lift coefficient C_L. It is

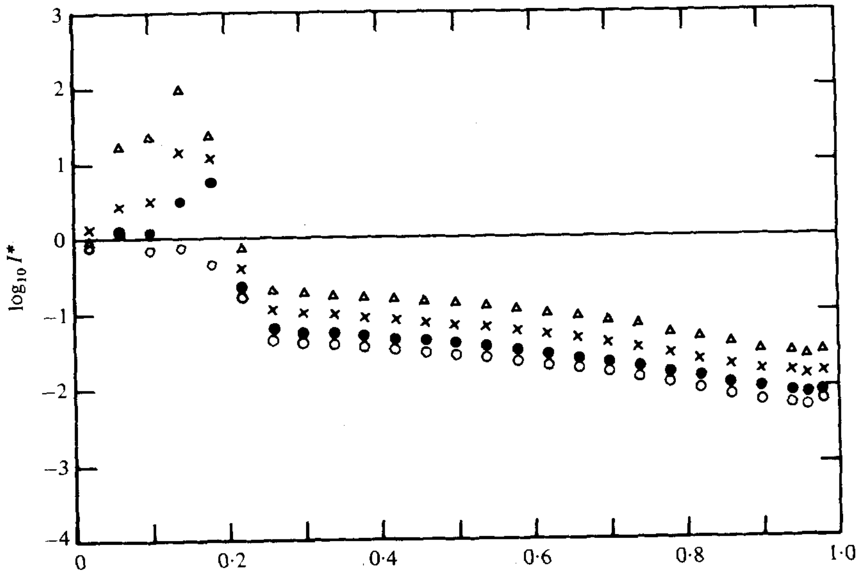

FIGURE 5. Values of I^* plotted against similarity ratio ϕ, in the case of an elliptic cylinder of thickness ratio $t = 0{\cdot}1$ inclined at $\alpha = 0°$. ○, $Re = 0{\cdot}01$; ●, $Re = 0{\cdot}1$; ×, $Re = 1$; △, $Re = 5$.

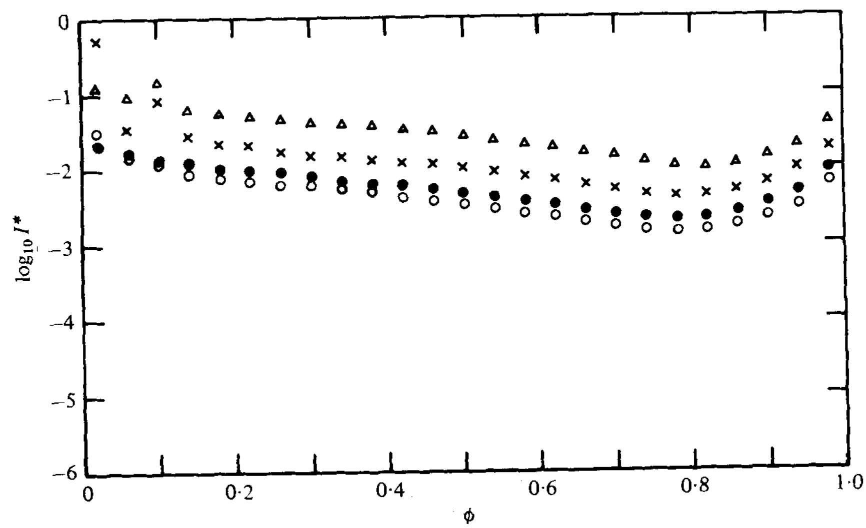

FIGURE 6. Values of I^* plotted against similarity ratio ϕ, in the case of an elliptic cylinder of thickness ratio $t = 0{\cdot}5$ inclined at $\alpha = 0°$. ○, $Re = 0{\cdot}01$; ●, $Re = 0{\cdot}1$; ×, $Re = 1$; △, $Re = 5$.

obvious from these plots that the drag and lift coefficients have maximum values at $\alpha = 90°$ and $\alpha = 45°$ respectively. And also, the data show that on the whole the present results agree fairly with Imai's, especially in the case of $Re = 0{\cdot}1$ and $t = 0{\cdot}5$.

Although our algorithm assumes the positions of singularities in the prescribed manner, we tried computations with the singularities distributed on the major axis of an ellipse. And it was observed that the rearrangement hardly affects the results. This will probably not always be the case, but it can be regarded as one of the desirable properties of the present technique.

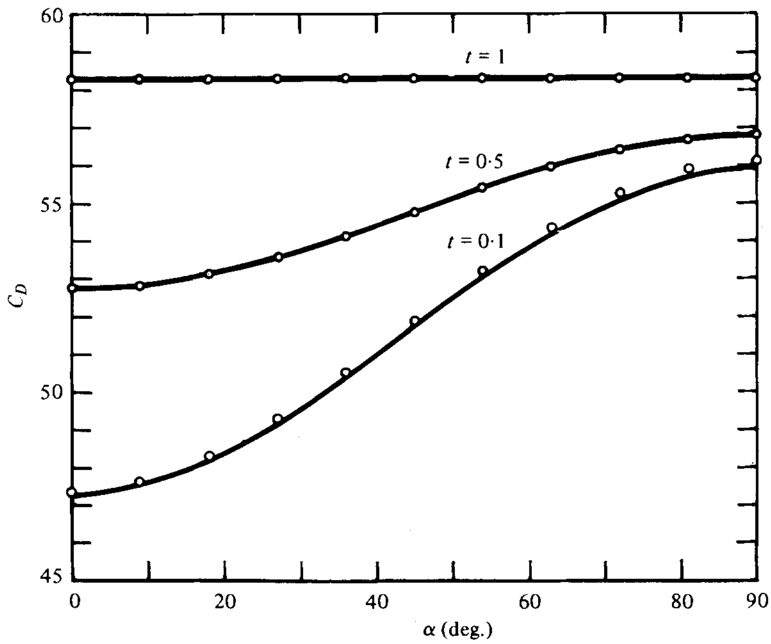

FIGURE 7. Drag coefficients C_D for inclined elliptic cylinders at $Re = 0{\cdot}1$, plotted against azimuthal angle α. t, thickness ratio b/a; ○, present results; ——, Imai's results (1954).

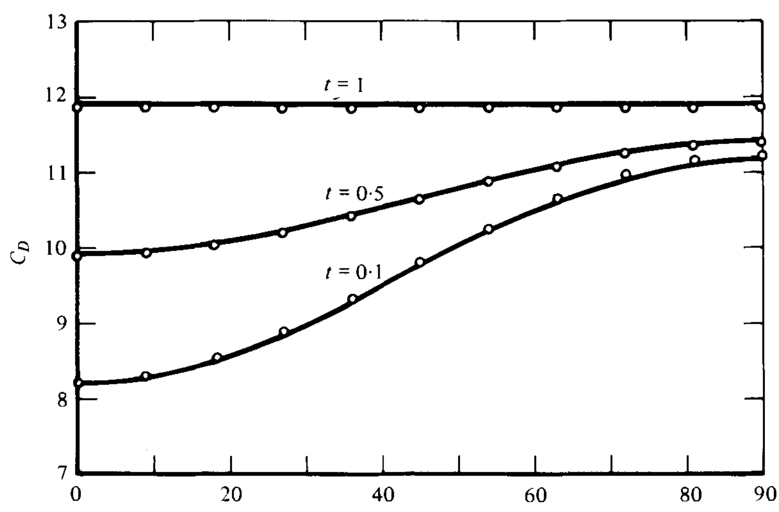

FIGURE 8. Drag coefficients C_D for inclined elliptic cylinders at $Re = 1$, plotted against azimuthal angle α. ○, present results; ——, Imai's results (1954).

Another point worthy of note concerns the fact that, for $Re \ll 1$, a certain well-known symmetry relationship that applies between the force and velocity in three-dimensional Stokes flows should also hold approximately in two-dimensional flows. Namely

$$k \equiv \frac{2C_L}{(C_{D2}-C_{D1})\sin 2\alpha} \simeq 1, \tag{4.8}$$

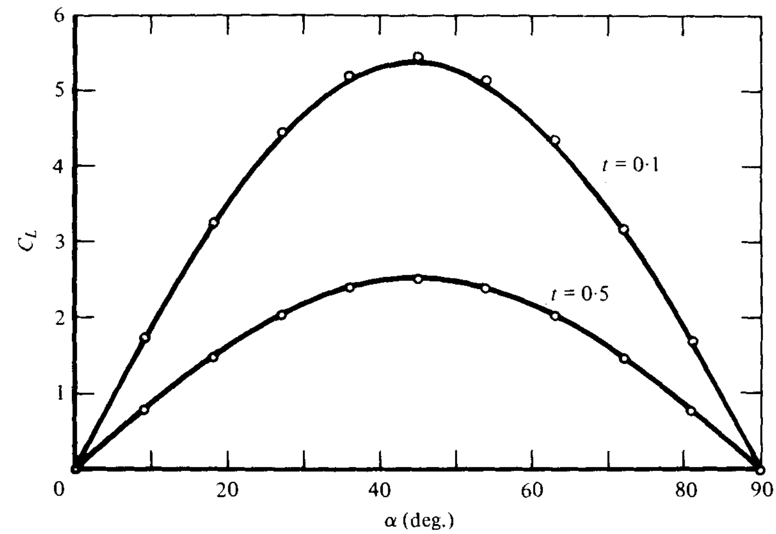

FIGURE 9. Lift coefficients C_L for inclined elliptic cylinders at $Re = 0{\cdot}1$, plotted against azimuthal angle α. ○, present results; ——, Imai's results (1954).

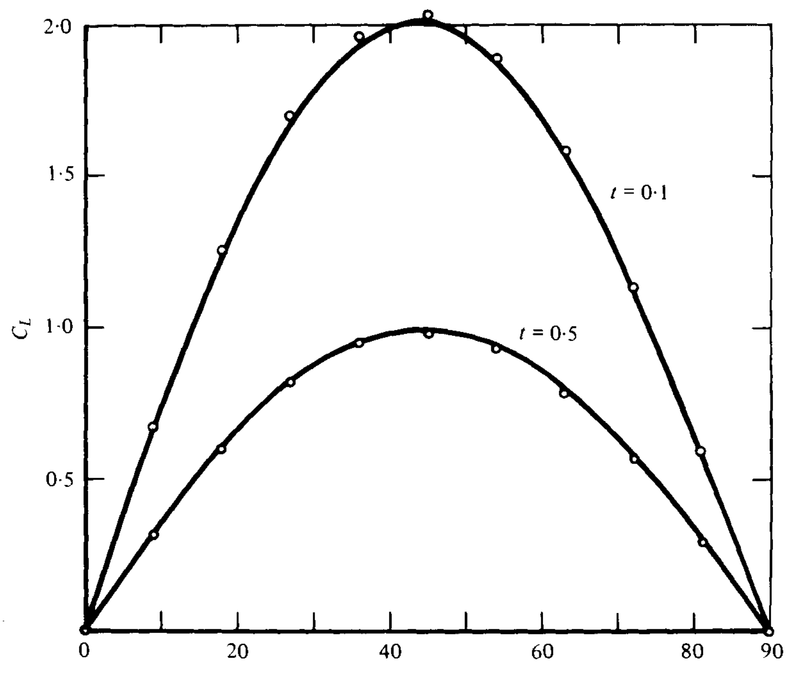

FIGURE 10. Lift coefficients C_L for inclined elliptic cylinders at $Re = 1$, plotted against azimuthal angle α. ○, present results; ——, Imai's results (1954).

where C_{D1} and C_{D2} are the drag coefficients at $\alpha = 0°$ and $90°$ respectively. From Imai (1954), we get

$$k = \frac{(2T+\sigma^2)(2T-\sigma^2)}{4T(T-1)-\sigma^2(\sigma^2+2\cos 2\alpha)}, \tag{4.9}$$

with

$$\sigma = (1-t)/(1+t),$$

and

$$T = \ln\{8(1+\sigma^2)/Re\}+\tfrac{1}{2}-\gamma.$$

Hence, it is obvious that

$$\lim_{Re\to 0} k = 1.$$

However, both the equation (4.9) and the present results indicate that this limiting behaviour can be reached only very close to $Re = 0$. For example, for $Re = 0{\cdot}1$, $t = 0{\cdot}1$ and $\alpha = 45°$, (4.9) yields

$$k = 1{\cdot}259,$$

whereas our method gives

$$k = 1{\cdot}250.$$

Furthermore, by virtue of (3.31) and (3.32) with figures 5 and 6, it can be found that the data in figures 7 and 9 contain errors of the orders of 0·03 for $t = 0{\cdot}1$, and 0·01 for $t = 0{\cdot}5$, and that the data in figures 8 and 10 contain errors of the orders of 0·06 for $t = 0{\cdot}1$, and 0·02 for $t = 0{\cdot}5$.

Considering both the above-mentioned error estimation and the numerical comparison with Imai's results (1954) which are correct to the order of Re according to his discussion, the present results can be recognized to be sufficiently accurate, so long as we are concerned with Oseen flows.

4.3. *Forces acting on two circular cylinders*

We consider two circular cylinders C_1 and C_2 of the same radius a which are immersed in a uniform flow field, as is shown in figure 11. Let $2h$ be the distance between their centres, and α be the angle between the x axis and the line passing through these centres. Our purpose is to calculate the drag and lift experienced by the cylinder C_1 with various values of α and h/a.

In this case, with composite singularities illustrated in figure 11, we employ a criterion integral in the form

$$I = \oint_{C_1} W\overline{W}\,ds + \oint_{C_2} W\overline{W}\,dS. \tag{4.10}$$

Then, values of I^* are computed for various values of α, $1 \leqslant h/a \leqslant 10$, $0 < \phi < 1$, and $0{\cdot}01 \leqslant Re \leqslant 5$, where $\phi = \delta/a$ and $Re = 2aU_\infty/\nu$. The results clearly show that the optimum value of ϕ hardly depends on any of these parameters in the specified ranges in a similar way as before, though evident data are omitted in the present paper.

Under various conditions with the optimum value $\phi = 0{\cdot}3$, we calculated the drag and lift coefficients C_D and C_L based on $l = 2a$ and $\beta = 1$ in (3.26) and (3.27). Figure 12 shows computed values of C_D/C_D^* for $h/a = 10$, $\alpha = 0°$, $90°$ and $180°$, and Re ranging

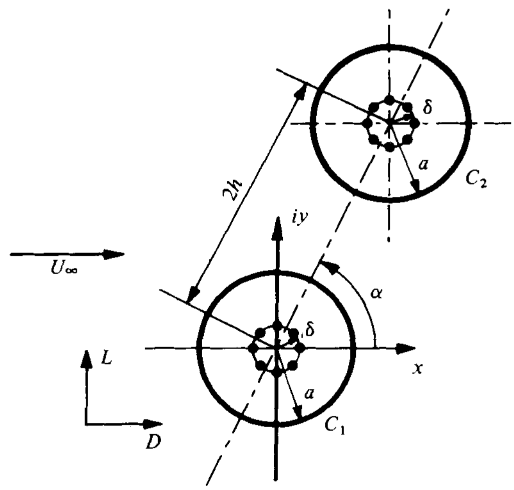

FIGURE 11. Flow past two circular cylinders of the same radius. ●, position of a composite singularity.

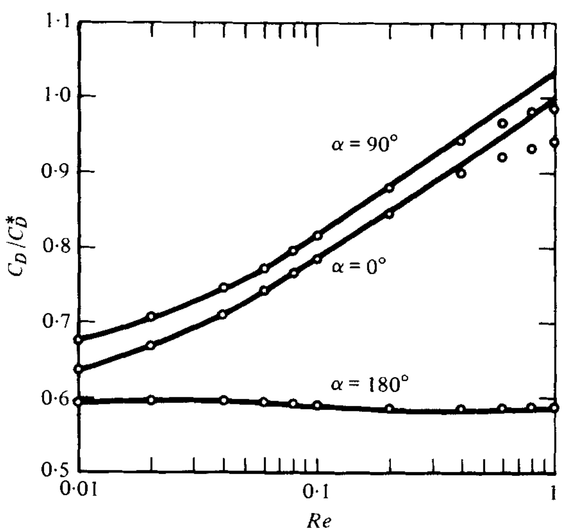

FIGURE 12. Relative drag coefficients C_D/C_D^* for the circular cylinder C_1 shown in figure 11 with $h/a = 10$. C_D^*, drag coefficient for a single circular cylinder calculated from (4.3); ○, present results; ——, Fujikawa's results (1956).

from 0·01 to 1·0, where C_D^* denotes the drag coefficient for a single circular cylinder given by (4.3). It is observed that on the whole the present results agree well with Fujikawa's (1956), which are correct to the order of Re^{-1}. Additionally, it is noticeable that the limiting behaviour clarified by Fujikawa (1956), namely

$$\lim_{Re\to 0} \frac{C_D}{C_D^*} = \tfrac{1}{2}, \tag{4.11}$$

for a finite value of h/a, is not well reached even at as small a Reynolds number as $Re = 0{\cdot}01$.

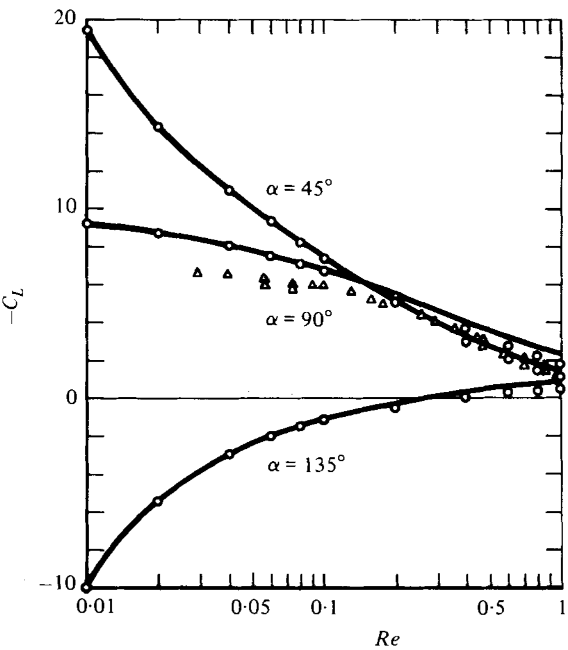

FIGURE 13. Lift coefficients C_L for the circular cylinder C_1 shown in figure 11 with $h/a = 10$. ——, Fujikawa's results (1956); ○, present results; △, Taneda's experiment (1957).

This characteristic is quite different from that of a Stokes flow past two spheres, because the value of C_D/C_D^* for one of them is independent of the body Reynolds number as described in the book of Happel & Brenner (1973). Besides, the results for $\alpha = 0°$ are significantly higher than those for $\alpha = 180°$, since the effect of wake of the interfering cylinder occurs in the case of $\alpha = 180°$. This also does not occur in a Stokes flow past two spheres.

Figure 13 shows computed values of C_L for $h/a = 10$ with $\alpha = 45°$, $90°$ and $135°$, compared with Fujikawa's results and Taneda's experimental data (1957) only for $\alpha = 90°$. It is noted that the cylinder C_1 always experiences a repulsive lift except for the case of $\alpha = 135°$ at lower Reynolds numbers. And also, there are fairly good agreements between the present computations, Fujikawa's theory and Taneda's experiments. Moreover, these data show basically different features from those of a Stokes flow past two spheres. That is, in the case of a Stokes flow, C_L does not depend on the body Reynolds number, having the same absolute value for $\alpha = 45°$ and $135°$, and vanishing at $\alpha = 90°$, as is mentioned in the book of Happel & Brenner (1973).

Furthermore, figures 14 and 15 respectively show variations of C_D/C_D^* and C_L with the distance ratio h/a in the case of $\alpha = 90°$, being compared with Fujikawa's results (1956, 1957). According to Fujikawa (1956)

$$\lim_{h/a\to\infty} \frac{C_D}{C_D^*} = 1. \tag{4.12}$$

However, as is obvious from figure 14, for $Re = 0{\cdot}1$ this limiting behaviour is not reached in practice even at as great a distance ratio as $h/a = 15$.

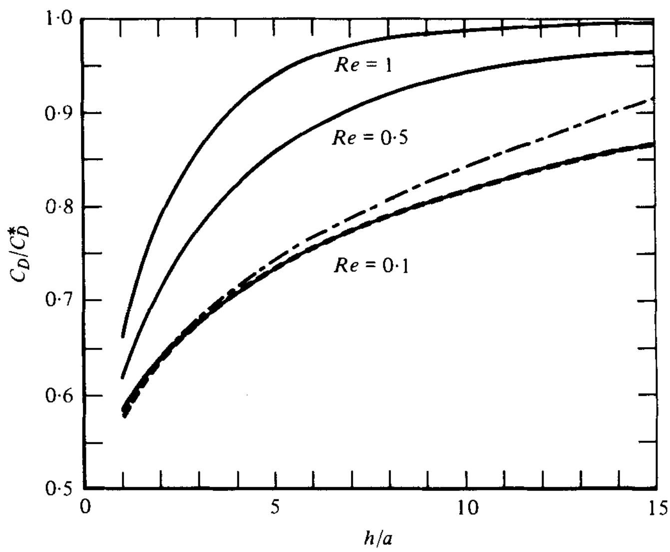

FIGURE 14. Relative drag coefficients C_D/C_D^* for the circular cylinder C_1 shown in figure 11, plotted against distance ratio h/a with $\alpha = 90°$. ——, present results; ------, Fujikawa's results (1956) with the assumption $\lambda h = O(1)$; —-—, Fujikawa's results (1957) with the assumption $\lambda h \ll 1$.

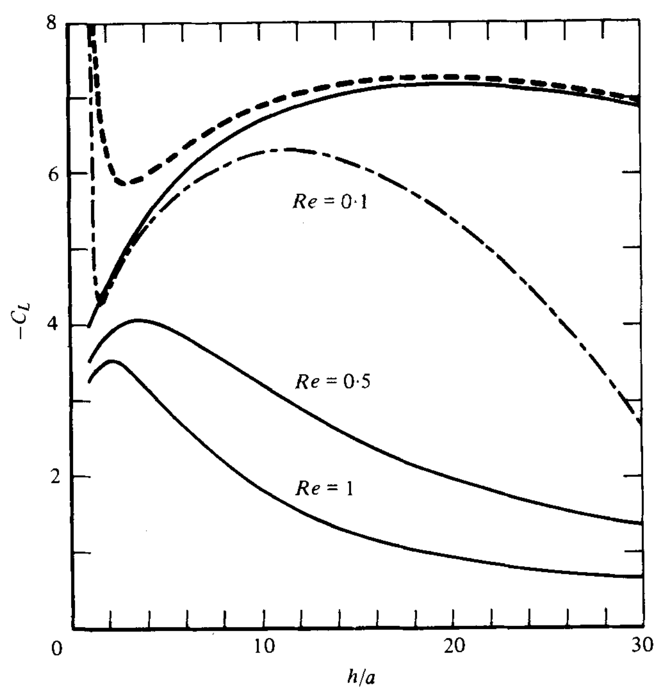

FIGURE 15. Lift coefficients C_L for the circular cylinder C_1 shown in figure 11, plotted against distance ratio h/a with $\alpha = 90°$. ——, present results; ------, Fujikawa's results (1956) with the assumption $\lambda h = O(1)$; —-—, Fujikawa's results (1957) with the assumption $\lambda h \ll 1$.

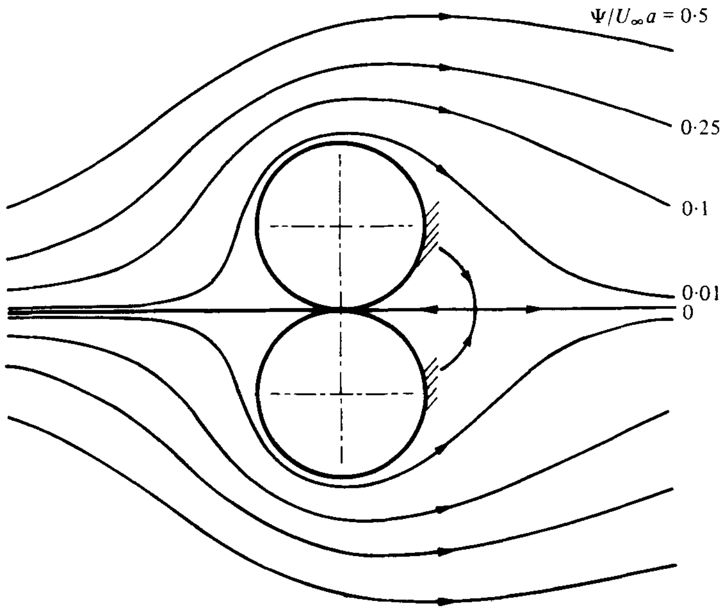

FIGURE 16. Flow pattern around two circular cylinders with $\alpha = 90°$ and $h/a = 1$ at $Re = 1$. Ψ, stream function; hatching indicating the regions where accurate streamlines cannot be expected.

On the other hand, the value of C_L in figure 15 shows somewhat complicated variations with maxima. And it can be found that generally the present results agree well with Fujikawa's (1957) at smaller values of h/a, and with Fujikawa's (1956) at larger values of h/a, on account of their assumptions $\lambda h = O(1)$ and $\lambda h \ll 1$ respectively. Further, there is a remarkable discrepancy between the present results and Fujikawa's (1957) near $h/a = 1$ because of the error term of $O(a^6/h^6)$ in his expansion formula.

To examine the general flow situations around the cylinders, we calculated the flow patterns for the cases of $\alpha = 90°$ and $Re = 1$ with $h/a = 1$, $1{\cdot}3$ and $2{\cdot}1$, the last one giving nearly a maximum value of C_L. The results are plotted in figures 16–18. The hatching indicates regions where accurate streamlines cannot be expected in the present method. As is observed in figure 16, when the cylinders are in contact, a very weak vortex region with vorticity as low as $5 \times 10^{-3} U_\infty/a$ occurs behind the cylinders. And it is likely that a smaller vortex region also exists on the upstream side, but our method is not accurate enough to identify it. When the cylinders are separated by a slight distance of $h/a = 1{\cdot}3$, a very low speed flow takes place between them, as is illustrated in figure 17. These flow patterns are generally expected ones, though there are no data for comparison.

Additionally, our error estimation with (3.31) and (3.32) indicated that the data in figures 12–15 contain errors ΔC_D and ΔC_L of the orders of less than 10^{-3} for $h/a = 1$, less than 5×10^{-5} for $h/a = 2$, and less than 10^{-5} for $h/a = 10$. Though a further examination is needed, the present results for drag and lift coefficients can be understood to be sufficiently accurate.

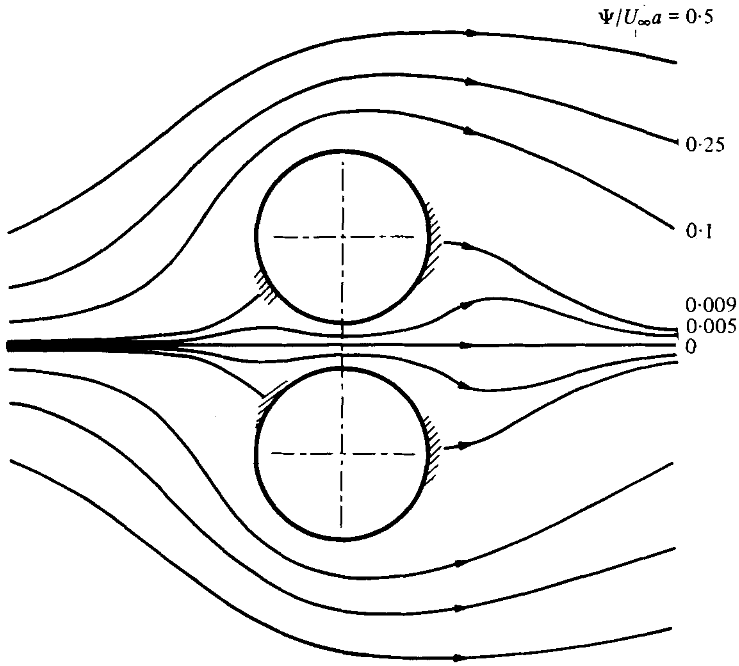

FIGURE 17. Flow pattern around two circular cylinders with $\alpha = 90°$ and $h/a = 1{\cdot}3$ at $Re = 1$.

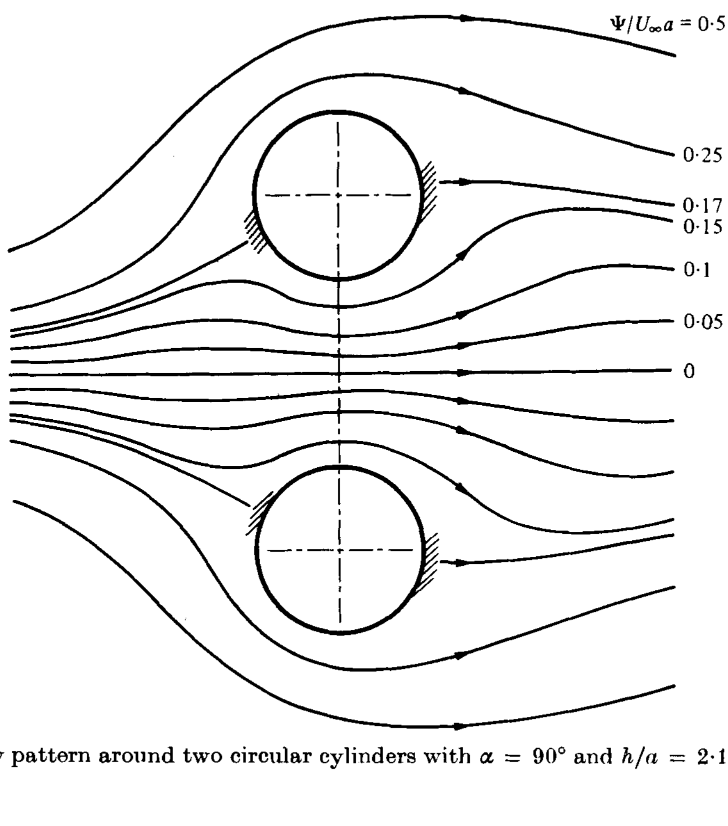

FIGURE 18. Flow pattern around two circular cylinders with $\alpha = 90°$ and $h/a = 2{\cdot}1$ at $Re = 1$.

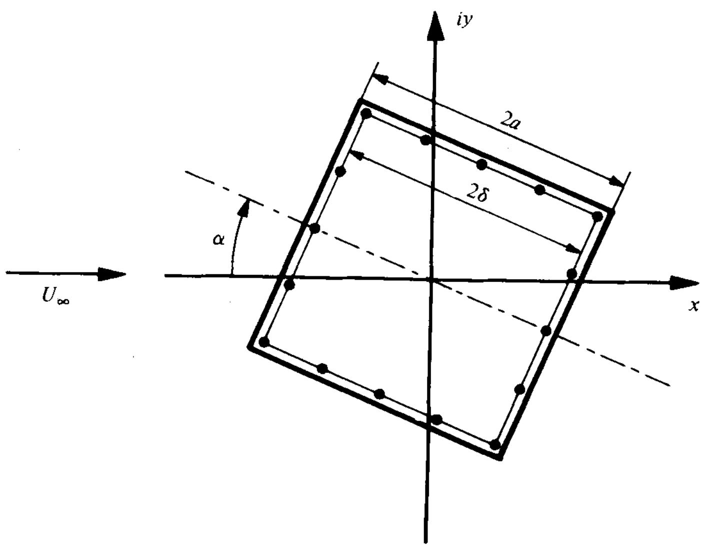

FIGURE 19. Flow past an inclined square cylinder. ●, position of a composite singularity.

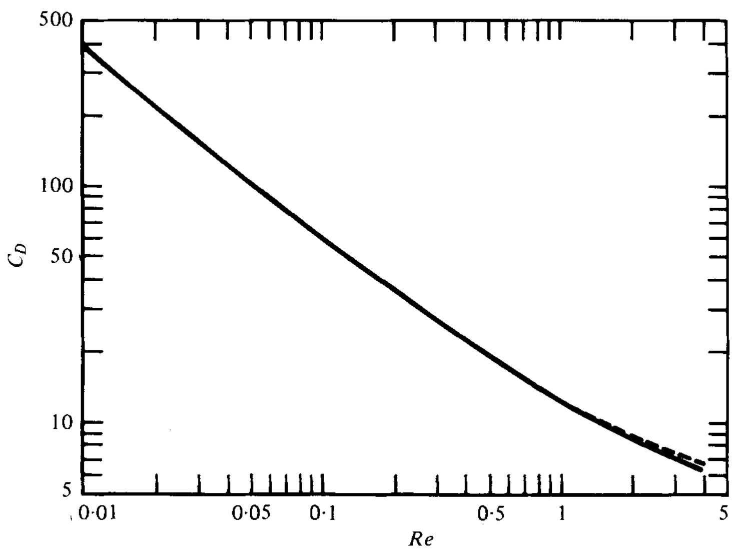

FIGURE 20. Drag coefficients C_D for an inclined square cylinder, plotted against Reynolds number Re. ——, $\alpha = 0°$; ------, $\alpha = 45°$.

4.4. *Forces acting on an inclined square cylinder*

We consider a single square cylinder of sides $2a$ inclined at angle α in a uniform flow field as is illustrated in figure 19. Similarly as before, our simulations with sixteen composite singularities showed that the optimum similarity ratio $\phi = \delta/a$ hardly depends on α and Re within a range of $0{\cdot}01 \leqslant Re \leqslant 5$, where $Re = 2aU_\infty/\nu$, though the data of them are omitted in the present paper.

With $\phi = 0{\cdot}93$, we computed the drag and lift coefficients C_D and C_L based on $l = 2a$ and $\beta = 1$ in (3.26) and (3.27). Figure 20 shows computed values of C_D for $\alpha = 0°$ and

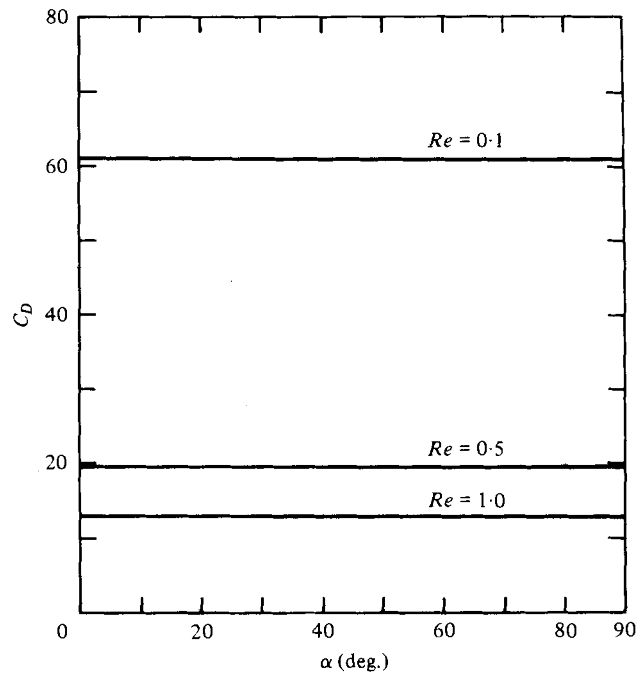

FIGURE 21. Variations of drag coefficient C_D with azimuthal angle α for the case of an inclined square cylinder.

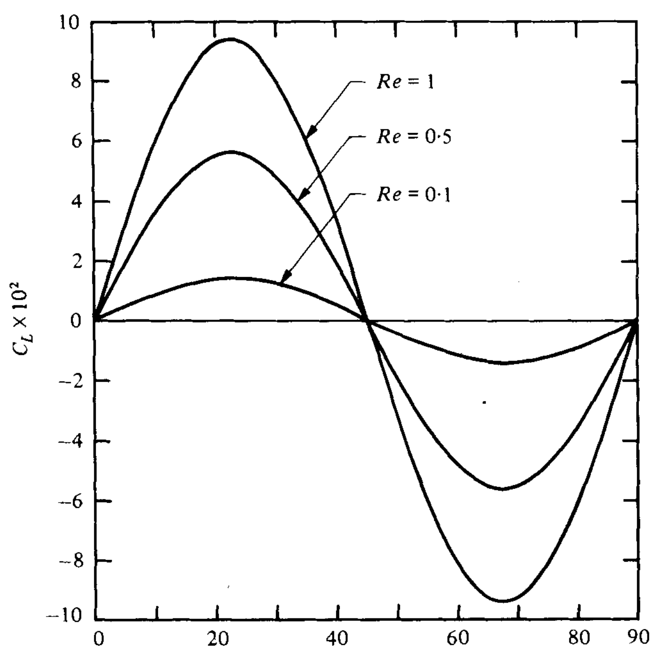

FIGURE 22. Variations of lift coefficient C_L with azimuthal angle α for the case of an inclined square cylinder.

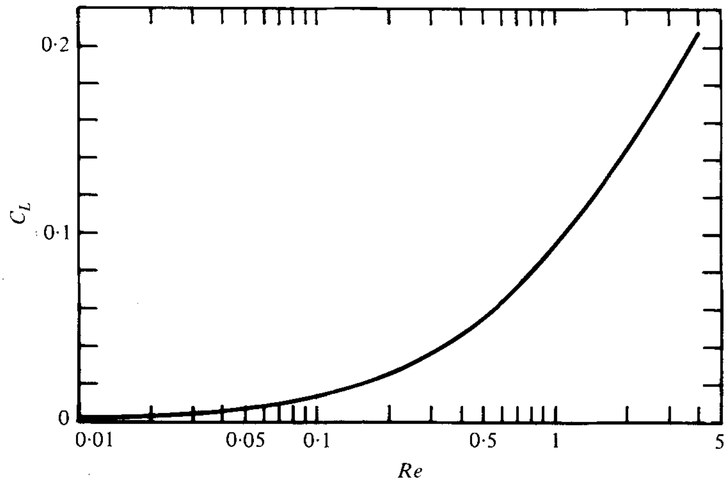

FIGURE 23. Lift coefficients C_L for a square cylinder inclined at $\alpha = 22{\cdot}5°$, plotted against Reynolds number Re.

45° with the Reynolds number Re ranging from 0·01 to 4. It is observed that the variations of C_D for both angles are similar to that of a single circular cylinder as is generally expected, and that a slight difference occurs between both cases as the Reynolds number Re increases.

Figures 21 and 22 illustrate respectively computed values of C_D and C_L for $Re = 0{\cdot}1$, 0·5 and 1·0, with the angle α ranging from 0° to 90°. These data reveal that the values of C_D are almost independent of α, and those of C_L are very small, the sign being switched at $\alpha = 45°$, and also extreme values occurring at $\alpha = 22{\cdot}5°$ and $67{\cdot}5°$.

Furthermore, figure 23 indicates variations of C_L at $\alpha = 22{\cdot}5°$ with the Reynolds number Re. Such slight values are not expected to be obtained in the finite difference method nor in the finite element method with so small a system of linear equations as are involved in the present formulation. Moreover, the data clearly indicate that the lift coefficient C_L increases with the Reynolds number Re within the presented range.

We tried a computation with another mode of singularity distribution, namely with singularities which are located diagonally inside the obstacle. And it was found that the rearrangement hardly affects the results, like the case of an elliptic cylinder.

Lastly, our error estimation made it clear that the data in figures 20–23 contain errors ΔC_D and ΔC_L of the orders of 0·03, 0·03 and 0·1 for $Re = 0{\cdot}01$, 0·1 and 1·0 respectively. Therefore, the values of C_D in figures 20 and 21 are considered comparatively accurate, but those of C_L in figures 22 and 23 are less acceptable so long as the present error estimation is valid. The errors in these data should be further examined from another point of view.

5. Conclusions

An approximate numerical method was proposed for solving the two-dimensional Oseen's linearized equations for flows past arbitrary cylindrical obstacles. As was already mentioned, the approach is based on a discrete singularity formulation with a least squares criterion for no-slip boundary condition, which is really an extension of the approximate method for two-dimensional potential flow problems proposed by the present authors Kieda & Yano (1978), and thus it falls within the so-called method of weighted residuals.

The present approach appears to have considerable promise as a technique for flow problems in complicated geometries that cannot be solved using classical analytical methods, and also it requires a much simpler computation algorithm with a relatively smaller system of linear equations than needed in the finite difference method, finite element method and continuous singularity method. Especially, our approach offers an analytical form of the approximate solution which is easier to treat than such one that can be obtained in the continuous singularity technique.

It is also noticeable that, in all cases of the present simulations, the optimum similarity ratio ϕ which specifies the most suitable positions of singularities hardly depends on the Reynolds number and the angular position of the body in question. This is very favourable for the present formulation.

Moreover, the rough error estimation for computed drag and lift coefficients proposed in this paper should be further examined for its validity from another point of view. Particularly in the case of an inclined square cylinder, a more critical error estimation is required for the computed lift coefficients.

Lastly, it should be added that all computations were performed on a FACOM M-190 computer in double precision (64 bits per floating point word).

REFERENCES

BAIRSTOW, L. 1923 The resistance of a cylinder moving in a viscous fluid. *Phil. Trans. Roy. Soc.* A **223**, 383–432.

FAXÉN, H. 1927 Exakte Lösung der oseenschen Differential-Gleichungen einer zähen Flussigkeit für den Fall der Translations-Bewegung eines Zylinders. *Nova Acta Soc. Sci. Upsal.*, vol. extra ord., 1–55.

FILON, L. N. G. 1926 The forces on a cylinder in a stream of viscous fluid. *Proc. Roy. Soc.* A **113**, 7–27.

FUJIKAWA, H. 1956 The forces acting on two circular cylinders of arbitrary radii placed in a uniform stream at low values of Reynolds number. *J. Phys. Soc. Japan* **11**, 690–701.

FUJIKAWA, H. 1957 Expansion formulae for the forces acting on two equal circular cylinders placed in a uniform stream at low values of Reynolds number. *J. Phys. Soc. Japan* **12**, 423–430.

HAPPEL, J. & BRENNER, H. 1973 *Low Reynolds Number Hydrodynamics*. Noordhoff.

HESS, J. L. & SMITH, A. M. O. 1966 Calculation of potential flow about arbitrary bodies. *Prog. Aero. Sci.* **8**, 1–138.

IMAI, I. 1951 On the asymptotic behaviour of viscous fluid flow at a great distance from a cylindrical body, with special reference to Filon's paradox. *Proc. Roy. Soc.* A **208**, 487–516.

IMAI, I. 1954 A new method of solving Oseen's equations and its application to the flow past an inclined elliptic cylinder. *Proc. Roy. Soc.* A **224**, 141–160.

KAPLUN, S. 1957 Low Reynolds number flow past a circular cylinder. *J. Math. Mech.* **6**, 595–603.

KIEDA, A. & YANO, H. 1978 Approximate numerical solutions for two-dimensional potential flow problems. *Trans. A.S.M.E., J. Fluids Engng* **100**, 122–124.

LAMB, H. 1911 On the uniform motion of a sphere through a viscous fluid. *Phil. Mag.* (6) **21**, 112–121.

LAMB, H. 1932 *Hydrodynamics*. Cambridge University Press.

OSEEN, C. W. 1910 Über die Stokes'sche Formel und über eine verwandte Aufgabe in der Hydrodynamik. *Ark. Mat. Astronom. Phys.* **6**, 29.

ROSENHEAD, L. 1963 *Laminar Boundary Layers.* Oxford University Press.

TANEDA, S. 1957 Experimental studies of the lift on two equal circular cylinders placed side by side in a uniform stream at low Reynolds numbers. *J. Phys. Soc. Japan* **12**, 419–422.

TOMOTIKA, S. & AOI, T. 1951 An expansion formula for the drag on a circular cylinder moving through a viscous fluid at small Reynolds numbers. *Quart. J. Mech. Appl. Math.* **4**, 401–406.

TRITTON, D. J. 1959 Experiments on the flow past a circular cylinder at low Reynolds numbers. *J. Fluid Mech.* **6**, 547–567.

VAN DYKE, M. 1964 *Perturbation Methods in Fluid Mechanics.* Academic.

YOUNGREN, G. K. & ACRIVOS, A. 1975 Stokes flow past a particle of arbitrary shape: a numerical method of solution. *J. Fluid Mech.* **69**, 377–403.